



## Momentum-resolved superconducting gap in the bulk of $\text{Ba}_{1-x}\text{K}_x\text{Fe}_2\text{As}_2$ from combined ARPES and $\mu\text{SR}$ measurements

To cite this article: D V Evtushinsky *et al* 2009 *New J. Phys.* **11** 055069

View the [article online](#) for updates and enhancements.

### Related content

- [Fe-based superconductors: an ARPES perspective](#)  
P Richard, T Sato, K Nakayama *et al.*
- [Probing the multi gap behavior within '11' and '122' families of iron based superconductors: the muon-spin rotation studies](#)  
R Khasanov and Z Guguchia
- [Strong nodeless pairing in \(Tl, K\)Fe1.78Se2](#)  
X.-P. Wang, T. Qian, P. Richard *et al.*

### Recent citations

- [In-plane magnetic penetration depth of superconducting  \$\text{CaKFe}\_4\text{As}\_4\$](#)   
Rustem Khasanov *et al*
- [Structure and Anisotropy of the Superconducting Order Parameter in  \$\text{Ba}\_{0.65}\text{K}\_{0.35}\text{Fe}\_2\text{As}\_2\$  Probed by Andreev Spectroscopy](#)  
T. E. Kuzmicheva *et al*
- [Phase-Sensitive Evidence for the Sign-Reversal  \$s\_{\pm}\$  Symmetry of the Order Parameter in an Iron-Pnictide Superconductor Using  \$\text{Nb}/\text{Ba}\_{1-x}\text{NaxFe}\_2\text{As}\_2\$  Josephson Junctions](#)  
A. A. Kalenyuk *et al*

## Momentum-resolved superconducting gap in the bulk of $\text{Ba}_{1-x}\text{K}_x\text{Fe}_2\text{As}_2$ from combined ARPES and $\mu\text{SR}$ measurements

D V Evtushinsky<sup>1,9</sup>, D S Inosov<sup>1,2</sup>, V B Zabolotnyy<sup>1</sup>,  
M S Viazovska<sup>3</sup>, R Khasanov<sup>4</sup>, A Amato<sup>4</sup>, H-H Klauss<sup>5</sup>,  
H Luetkens<sup>4</sup>, Ch Niedermayer<sup>6</sup>, G L Sun<sup>2</sup>, V Hinkov<sup>2</sup>, C T Lin<sup>2</sup>,  
A Varykhalov<sup>7</sup>, A Koitzsch<sup>1</sup>, M Knupfer<sup>1</sup>, B Büchner<sup>1</sup>,  
A A Kordyuk<sup>1,8</sup> and S V Borisenko<sup>1</sup>

<sup>1</sup> Institute for Solid State Research, IFW Dresden, PO Box 270116,  
D-01171 Dresden, Germany

<sup>2</sup> Max-Planck-Institute for Solid State Research, Heisenbergstrasse 1,  
D-70569 Stuttgart, Germany

<sup>3</sup> Max-Planck-Institute for Mathematics, Vivatsgasse 7, 53111 Bonn, Germany

<sup>4</sup> Laboratory for Muon Spin Spectroscopy, Paul Scherrer Institut,  
CH-5232 Villigen PSI, Switzerland

<sup>5</sup> IFP, TU Dresden, D-01069 Dresden, Germany

<sup>6</sup> Laboratory for Neutron Scattering, Paul Scherrer Institute and ETH  
Zürich, CH-5232 Villigen PSI, Switzerland

<sup>7</sup> BESSY GmbH, Albert-Einstein-Strasse 15, 12489 Berlin, Germany

<sup>8</sup> Institute of Metal Physics of National Academy of Sciences of Ukraine,  
03142 Kyiv, Ukraine

E-mail: [danevt@gmail.com](mailto:danevt@gmail.com)

*New Journal of Physics* **11** (2009) 055069 (13pp)

Received 11 February 2009

Published 29 May 2009

Online at <http://www.njp.org/>

doi:10.1088/1367-2630/11/5/055069

**Abstract.** Here we present a calculation of the temperature-dependent London penetration depth,  $\lambda(T)$ , in  $\text{Ba}_{1-x}\text{K}_x\text{Fe}_2\text{As}_2$  (BKFA) on the basis of the electronic band structure (Zabolotnyy *et al* 2009 *Nature* **457** 569, Zabolotnyy *et al* 2009 *Physica C* **469** 448) and momentum-dependent superconducting gap (Evtushinsky *et al* 2009 *Phys. Rev. B* **79** 054517) extracted from angle-resolved photoemission spectroscopy (ARPES) data. The results are compared to the direct measurements of  $\lambda(T)$  by muon spin rotation ( $\mu\text{SR}$ ) (Khasanov

<sup>9</sup> Author to whom any correspondence should be addressed.

*et al* 2009 *Phys. Rev. Lett.* **102** 187005). The value of  $\lambda(T = 0)$ , calculated with no adjustable parameters, equals 270 nm, while the directly measured one is 320 nm; the temperature dependence  $\lambda(T)$  is also easily reproduced. Such agreement between the two completely different approaches allows us to conclude that ARPES studies of BKFA are bulk-representative. Our review of the available experimental studies of the superconducting gap in the new iron-based superconductors in general allows us to state that most of them bear two nearly isotropic gaps with coupling constants  $2\Delta/k_B T_c = 2.5 \pm 1.5$  and  $7 \pm 2$ .

## Contents

<b>1. Introduction</b>	<b>2</b>
<b>2. The London penetration depth from the electronic band structure</b>	<b>2</b>
<b>3. Low-energy electronic band structure of BKFA</b>	<b>3</b>
<b>4. Results</b>	<b>7</b>
<b>5. Experimental details</b>	<b>8</b>
<b>6. Overview of experimental studies of the gap in iron-based high-<math>T_c</math> superconductors</b>	<b>9</b>
<b>7. Conclusions</b>	<b>11</b>
<b>Acknowledgments</b>	<b>11</b>
<b>Appendix</b>	<b>11</b>
<b>References</b>	<b>12</b>

## 1. Introduction

The superconducting energy gap in the newly discovered iron-based superconductors naturally attracted much attention of physicists, and during one year of hard work, these materials were investigated by numerous experimental techniques [1]–[40]. As the diversity of conclusions made about the symmetry and value of the gap is huge, which can be attributed to the various shortcomings of different methods, the situation seems to be far from clear. In this paper, based on the angle resolved photoemission spectroscopy (ARPES) and muon spin rotation ( $\mu$ SR) data taken from the same single crystals of  $\text{Ba}_{1-x}\text{K}_x\text{Fe}_2\text{As}_2$  (BKFA) with  $T_c = 32$  K, we succeeded in revealing robust momentum dependence of the gap in this compound. The coupling constant,  $2\Delta/k_B T_c$ , is  $\simeq 1$  for the outer  $\Gamma$ -barrel and 6.8 for all other Fermi surface sheets. Furthermore, a close inspection of many studies of different iron-based superconductors allows one to derive quite definitive conclusions about the gap in these materials.

## 2. The London penetration depth from the electronic band structure

The London penetration depth,  $\lambda$ , can be expressed through the electronic band structure. For the quasi-two-dimensional superconductor with equivalent  $a$  and  $b$  principal axes, the formula, relating in-plane penetration depth to the band dispersion, reads (in SI units)

$$\frac{1}{\lambda^2(T)} = \frac{e^2}{2\pi \varepsilon_0 c^2 h L_c} \cdot \int_{\text{FS}} v_{\text{F}}(\mathbf{k}) \left[ 1 - \int_{-\infty}^{+\infty} \left( -\frac{\partial f_T(\omega)}{\partial \omega} \right) \left| \text{Re} \frac{\omega + i\Sigma''}{\sqrt{(\omega + i\Sigma'')^2 - \Delta_{\mathbf{k}}^2(T)}} \right| d\omega \right] dk, \quad (1)$$

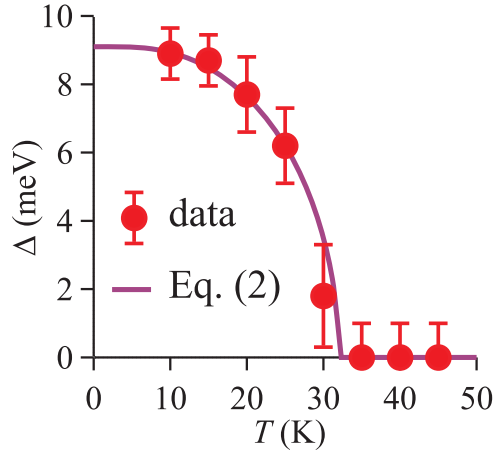


**Figure 1.** Temperature dependence of the superconducting gap in BKFA as extracted from ARPES spectra [3]. The underlying fitting curve is described by equation (2).

where  $\mathbf{k}$  is the quasimomentum,  $\omega$  is the energy,  $v_F$  is the Fermi velocity,  $\Delta_{\mathbf{k}}(T)$  is the momentum-dependent superconducting gap,  $\Sigma''$  is the scattering rate (in the following we assume clean limit,  $\Sigma'' = 0$ ),  $dk$  is the element of the Fermi surface length,  $T$  is the temperature,  $L_c$  is the size of the elementary cell along the  $c$ -axis,  $f_T(\omega) = [1 + \exp(\omega/k_B T)]^{-1}$  is the Fermi function,  $k_B$  is the Boltzmann constant,  $h$  is Planck's constant,  $\epsilon_0$  is the electric constant,  $c$  is the speed of light and  $e$  is the elementary charge<sup>10</sup>. Formula (1) is consistent with results already presented in the literature [41], although the former accounts for a finite lifetime, and for the four-fold symmetry of the problem (see also [42]).

### 3. Low-energy electronic band structure of BKFA

The information required to calculate  $\lambda(T)$  via formula (1) can be extracted directly from ARPES spectra. The temperature and momentum dependence of the superconducting gap were obtained in [3], and the band structure was qualitatively revealed in [1, 2]. The momentum dependence of the superconducting gap is quite easy to describe—the gap is large,  $\Delta_{\mathbf{k}}(T) = \Delta_{\text{large}}(T)$ , on the inner  $\Gamma$ -barrel and the propeller-like structure around the X point, and it is small,  $\Delta_{\mathbf{k}}(T) = \Delta_{\text{small}}(T)$ , on the outer  $\Gamma$ -barrel. The temperature dependence of the gap (see figure 1) is well fitted by the formula<sup>11</sup>

$$\Delta_{\text{large,small}}(T) = \Delta_{\text{large,small}}(0) \cdot \tanh\left(\frac{\pi}{2} \cdot \sqrt{\frac{T_c}{T} - 1}\right) \quad (2)$$

with  $\Delta_{\text{large}}(0) = 9.1$  meV and  $\Delta_{\text{small}}(0) < 4$  meV.

<sup>10</sup> Note that in the simplest case of round Fermi surface and zero temperature, equation (1) yields a well-known formula:  $\lambda^2 = \epsilon_0 m c^2 / n e^2$  (or  $\lambda^2 = c^2 m / 4\pi n e^2$  in CGS units), where  $n = (2\pi^2 L_c)^{-1} \int f(\epsilon(\mathbf{k})) d^2\mathbf{k}$  and  $m = \hbar k_F / v_F$ .

<sup>11</sup> To the best of our knowledge, this formula was suggested in [43].

Taking into account the mentioned momentum dependence of the gap, one can rewrite (1) in the following way:

$$\frac{1}{\lambda^2(T)} = I_1 [1 - D(\Delta_{\text{large}}(T), \Sigma'', T)] + I_2 [1 - D(\Delta_{\text{small}}(T), \Sigma'', T)], \quad (3)$$

where  $I_{1,2}$  are temperature-independent factors<sup>12</sup>

$$I_1 = \frac{e^2}{2\pi \varepsilon_0 c^2 \hbar L_c} \int_{\substack{\text{outer } \Gamma, \\ \text{blades,} \\ \text{X-pocket}}} v_F(\mathbf{k}) d\mathbf{k}, \quad I_2 = \frac{e^2}{2\pi \varepsilon_0 c^2 \hbar L_c} \int_{\text{inner } \Gamma} v_F(\mathbf{k}) d\mathbf{k}, \quad (4)$$

and  $D(\Delta, \Sigma'', T)$  is defined as

$$D(\Delta, \Sigma'', T) \equiv \int_{-\infty}^{+\infty} \left( -\frac{\partial f_T(\omega)}{\partial \omega} \right) \left| \text{Re} \frac{\omega + i\Sigma''}{\sqrt{(\omega + i\Sigma'')^2 - \Delta^2}} \right| d\omega. \quad (5)$$

See the appendix for the evaluation of this integral.

In figure 2 we present a quantitative investigation of the low-lying electronic band structure of BKFA. The band dispersion is extracted from ARPES data taken at a temperature slightly above the superconducting transition. The Fermi velocities for the inner and outer  $\Gamma$ -barrels along the  $\Gamma X$  direction equal  $v_{i\Gamma}^{\Gamma X} = 0.51 \text{ eV } \text{\AA}$  and  $v_{o\Gamma}^{\Gamma X} = 0.36 \text{ eV } \text{\AA}$ , respectively (see figures 2(d)–(g) and (i)); along the  $\Gamma M$  direction, they are  $v_{i\Gamma}^{\Gamma M} = 0.54 \text{ eV } \text{\AA}$  and  $v_{o\Gamma}^{\Gamma M} = 0.43 \text{ eV } \text{\AA}$  (see figures 2(b), (c) and (h)), resulting in  $v_{i\Gamma} = 0.52 \text{ eV } \text{\AA}$  and  $v_{o\Gamma} = 0.40 \text{ eV } \text{\AA}$  on average. Fermi momenta for the inner and outer  $\Gamma$ -barrels are  $k_{i\Gamma} = 0.14 \text{ \AA}^{-1}$  and  $k_{o\Gamma} = 0.30 \text{ \AA}^{-1}$ , respectively (see figures 2(b)–(g) and (j)–(k)). Kinks in the dispersions of the inner and outer  $\Gamma$ -barrels around 25 meV have been described elsewhere [48]. For the electron-like X-pocket  $k_e = 0.06 \text{ \AA}^{-1}$ , and the depth of the band is  $\varepsilon_e = 17 \pm 3 \text{ meV}$  (see figures 3 and 4(b)), from where, assuming a parabolic band dispersion for this small pocket, we infer  $v_e = 2\varepsilon_e/\hbar k_e = 0.57 \text{ eV } \text{\AA}$ . For the hole-like blade pocket the average Fermi momentum equals  $k_h = 0.06 \text{ \AA}^{-1}$  and we estimate  $\varepsilon_h$  as 5–15 meV (see figure 4(b)); thus the average Fermi velocity equals  $v_h = 0.33 \text{ eV } \text{\AA}$ . The  $c$ -axis lattice constant equals 13.3  $\text{\AA}$  [44, 46].

The low-energy band dispersion can be well approximated by the following formulae:

1. inner  $\Gamma$ -barrel

$$\xi_{i\Gamma}(k_x, k_y) = 0.52 \left( 0.14 - \sqrt{\left(k_x + \frac{2\pi m}{L_a}\right)^2 + \left(k_y + \frac{2\pi n}{L_a}\right)^2} \right), \quad m, n \in \mathbb{Z}, \quad (6)$$

where  $L_a$  is the in-plane lattice constant, which according to [46, 48], equals 3.90  $\text{\AA}$ ;

2. outer  $\Gamma$ -barrel

$$\xi_{o\Gamma}(k_x, k_y) = 0.40 \left( 0.3 - \sqrt{\left(k_x + \frac{2\pi m}{L_a}\right)^2 + \left(k_y + \frac{2\pi n}{L_a}\right)^2} \right), \quad m, n \in \mathbb{Z}; \quad (7)$$

3. X-pocket

$$\xi_X(k_x, k_y) = 0.017 \left( \frac{\left[k_x + \frac{\pi(1+2m)}{L_a}\right]^2 + \left[k_y + \frac{\pi(1+2n)}{L_a}\right]^2}{0.06^2} - 1 \right), \quad m, n \in \mathbb{Z}; \quad (8)$$

<sup>12</sup> In this paper the calculations are carried out for two blade-pockets per Brillouin zone.

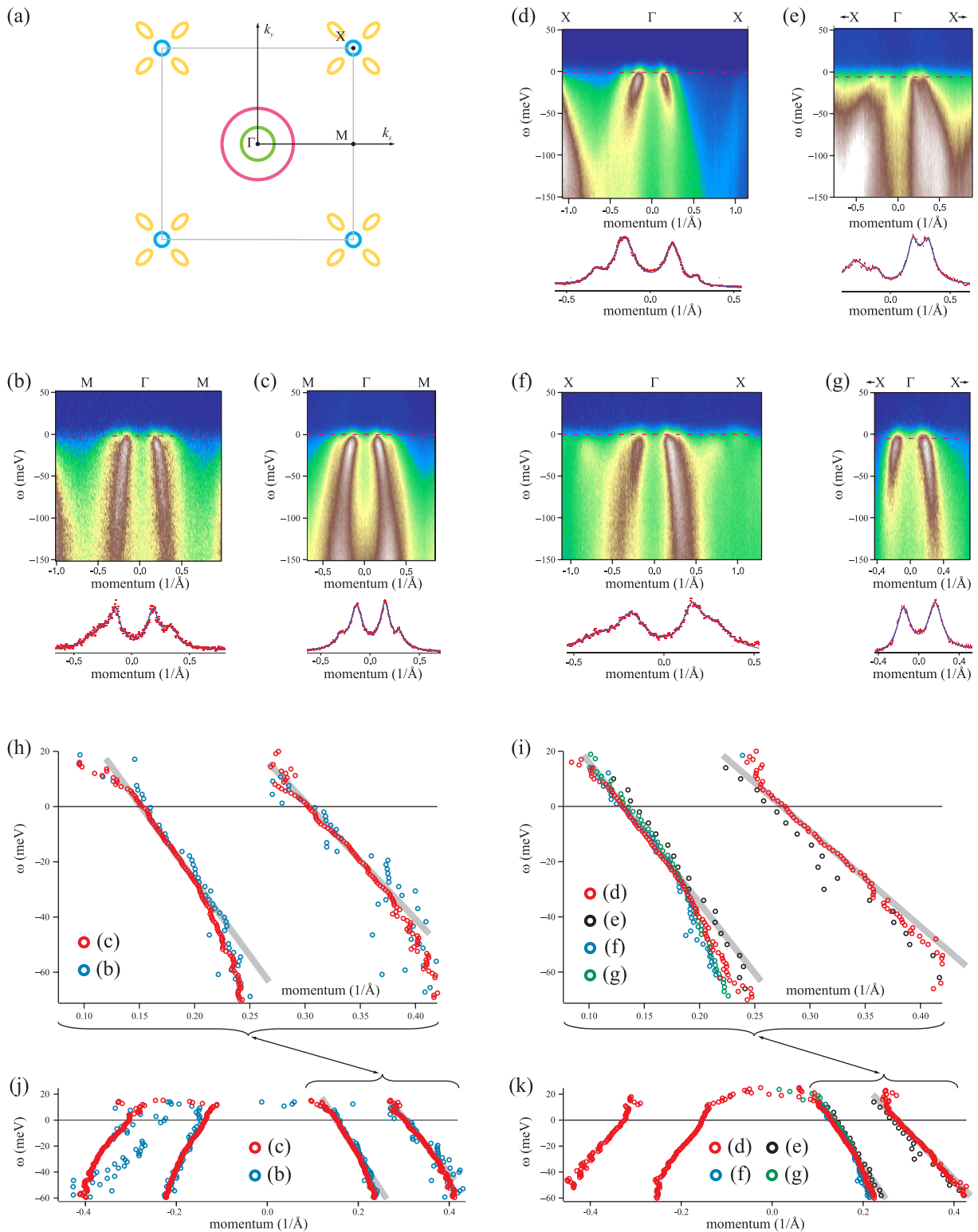


**Figure 2.** For caption see next page.

**Figure 2.** Determination of the low-energy band dispersion of BKFA from ARPES spectra. (a) Fermi surface of BKFA, as seen in ARPES [1]–[3]. Cuts along  $\Gamma M$ : (b)  $\Gamma_{-2,0}$  (index enumerates Mahan photoemission cones [45]),  $T = 36$  K,  $h\nu = 80$  eV, horizontal polarization; (c)  $\Gamma_{0,0}$ ,  $T = 45$  K,  $h\nu = 50$  eV, horizontal polarization. Cuts along  $\Gamma X$ : (d)  $\Gamma_{0,0}$ ,  $T = 35$  K,  $h\nu = 70$  eV, vertical polarization; (e)  $\Gamma_{+1,0}$ ,  $T = 35$  K,  $h\nu = 70$  eV, vertical polarization; (f)  $\Gamma_{0,0}$ ,  $T = 35$  K,  $h\nu = 80$  eV, horizontal polarization; (g)  $\Gamma_{0,0}$ ,  $T = 41$  K,  $h\nu = 40$  eV, vertical polarization. Blue corresponds to the minimum photoemission intensity, white to the maximum. Momentum distribution curves (MDC) taken nearly at the Fermi level are shown below each energy–momentum cut in order to demonstrate the high quality of the data and fits. Low-energy band dispersion of BKFA was extracted by an MDC fit from the data taken in different experimental conditions. The Fermi velocities and Fermi momenta can be determined from (h, i) and (j, k), respectively.

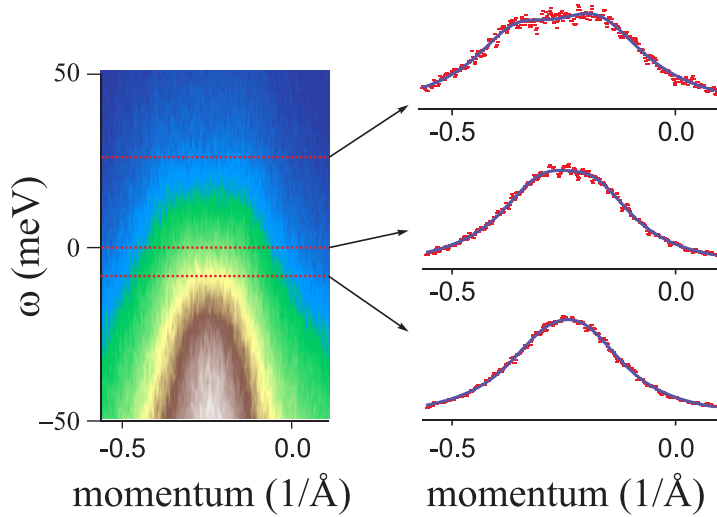


**Figure 3.** Dispersion of the X-pocket. The energy–momentum cut through the X point along  $\Gamma X$ ,  $T = 200$  K (left of the figure) and fit of the MDC to two Lorentzians (right). Measurements at high temperatures allow us to track band dispersion of the X pocket also above the Fermi level. The experimental conditions are such that the blades are suppressed due to photoemission matrix element effects.

#### 4. blades

$$\xi_b(k_x, k_y) = 0.01 \left( 1 - \left[ \frac{\frac{k_x + k_y}{\sqrt{2}} + \frac{\sqrt{2}\pi(1+2m)}{L_a} \pm 0.36}{0.08} \right]^2 - \left[ \frac{\frac{k_x - k_y}{\sqrt{2}} + \frac{\sqrt{2}\pi(1+2n)}{L_a}}{0.04} \right]^2 \right), \quad m, n \in \mathbb{Z}. \quad (9)$$

These dispersion relations are visualized in figure 4(c).

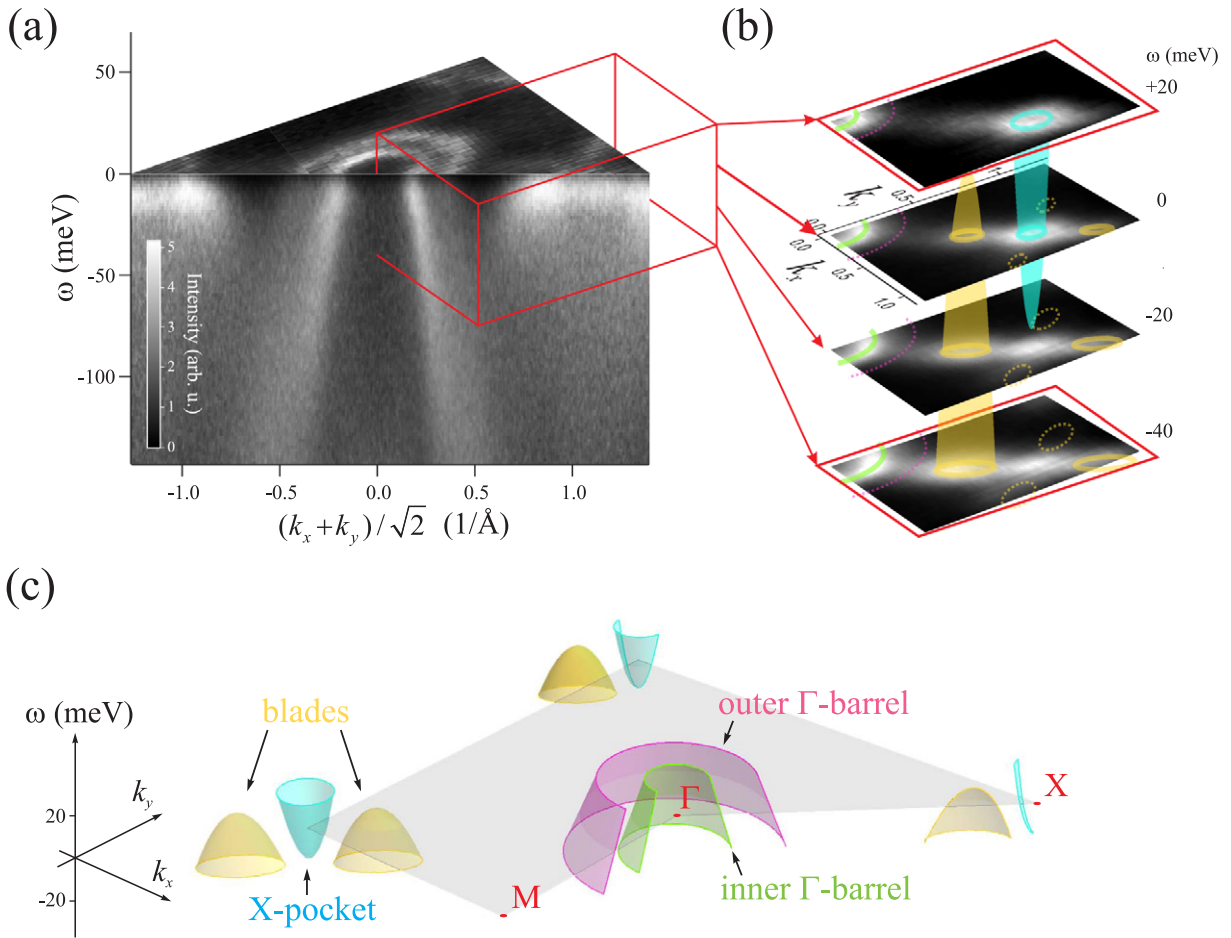


**Figure 4.** (a) A three-dimensional representation of the ARPES data. (b) The dispersion of the shallow bands near the X point can be determined from constant-energy cuts through the intensity distribution taken at different energies. The cross-section of the electron-like X pocket increases with energy, while the cross-section of the hole-like blades decreases. (c) The model for the low-energy band dispersion in BKFA, derived from ARPES data (figures 2, 3 and 4(b)).

#### 4. Results

The penetration depth at  $T \rightarrow 0$  in the clean limit depends only on the band structure and does not depend on the value of the superconducting gap (provided it is not zero) and, therefore, can be calculated purely from ARPES without any additional assumptions:

$$\frac{1}{\lambda^2(0)} = I_1 + I_2 = \frac{e^2}{2\pi \epsilon_0 c^2 h L_c} \left[ \int_{\text{inner } \Gamma} v_F(\mathbf{k}) dk + \int_{\text{outer } \Gamma} v_F(\mathbf{k}) dk + \int_{\text{X-pocket}} v_F(\mathbf{k}) dk + \int_{\text{blades}} v_F(\mathbf{k}) dk \right], \quad (10)$$

which results in  $\lambda(0) = 270$  nm.



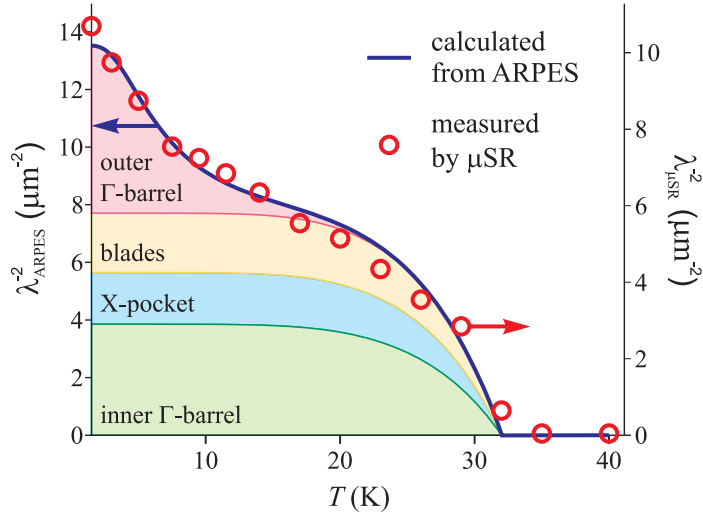


**Figure 5.** The in-plane London penetration depth in single crystals of BKFA as calculated from ARPES with one adjustable parameter,  $\Delta_{\text{small}}$ , and as measured directly by  $\mu\text{SR}$ . The temperature dependence of the normalized penetration depth is reproduced with the best accuracy for  $\Delta_{\text{small}} = 1.1$  meV, which is in agreement with our previous estimate  $\Delta_{\text{small}} < 4$  meV [3]. Contributions from different Fermi surface sheets are shown by different colors.

This is in remarkable agreement with the value of 320 nm obtained by muon spin rotation ( $\mu\text{SR}$ ) [4], the more so when one takes into account the complementarity of the two methods. The temperature variation of  $\lambda$  strongly depends on the values of the superconducting gap. Due to technical reasons, the small gap has not been determined precisely from ARPES measurements—only an upper limit of  $\Delta_{\text{small}} < 4$  meV was obtained [3]. Therefore, we use  $\Delta_{\text{small}}$  as a fitting parameter when comparing  $\lambda(T)$  calculated from ARPES with that determined from muon-spin depolarization rate in the  $\mu\text{SR}$  experiments (figure 5). The best fit of the normalized data corresponds to  $\Delta_{\text{small}} = 1.1$  meV. The good agreement between absolute values of  $\lambda$  at  $T = 0$  from ARPES (270 nm) and  $\mu\text{SR}$  (320 nm) implies correct determination of the band dispersion in the vicinity of the Fermi level. The possibility of fitting the normalized temperature dependence with only one fitting parameter implies (i) correct determination of the relative contributions from different Fermi surface sheets, (ii) perfect agreement between two independent experimental techniques concerning the value of  $\Delta_{\text{large}}$  and (iii) the possibility of improving the estimate of  $\Delta_{\text{small}}$  (now  $2\Delta_{\text{small}}/k_{\text{B}}T_{\text{c}} \simeq 1$ ) with respect to pure ARPES measurements ( $< 3$ ) [3]. The general good agreement between ARPES and  $\mu\text{SR}$  studies of BKFA allows us to state that ARPES experiments in this case are bulk-representative.

## 5. Experimental details

Single crystals of BKFA were grown using Sn as flux in a zirconia crucible. The growth details are described in [48]. The crystals were cleaved *in situ* and measured with a Scienta SES R4000 analyzer at the base pressure of  $5 \times 10^{-11}$  mbar. ARPES experiments were performed using the ‘1<sup>3</sup> ARPES’ end station at BESSY. Details of the experimental geometry can be found in [47].

**Table 1.** Coupling strength,  $2\Delta/k_B T_c$ , in iron-based superconductors, as revealed by different experimental techniques—compared with the BCS universal value 3.53. Most of the available studies reveal two superconducting gaps of different magnitudes, which are represented in the table as ‘large’ and ‘small’. References [5]–[12] are point contact Andreev reflection spectroscopy (PCAR) studies, [3], [13]–[18] are ARPES studies, [19] is a critical magnetic field ( $H_{c1}$ ) measurement, [4], [20]–[22] are  $\mu$ SR studies, [23] is an SI measurement, [24, 25] are optics spectroscopy studies, and [26]–[29] are STS studies.

Method	PCAR								ARPES						
	Ref. no.	[5]	[6]	[7]	[8]	[9]	[10]	[11]	[12]	[13]	[14]	[15]	[16]	[17]	[3]
Large gap	–	4.8	9.6	8.2	5.7	5.8	8.7	6.6	9	8.1	8.2	6.8	7.5	6.8	6.5
Small gap	3.7	1.7	3.4	2.8	2.6	–	2.7	2.6	–	3.6	5.5	–	3.9	<3	4.2

Method	$H_{c1}$	$\mu$ SR				SI	Optics		STS			
	Ref. no.	[19]	[20]	[4]	[21]	[22]	[23]	[24]	[25]	[26]	[27]	[28]
Large gap	5.8	7.3	6.7	4.5	7.2	4.8	7.5	8.2	–	7	7.4	5.7
Small gap	1.3	4.1	1.2	1.1	2.7	2.3	–	–	3.7	–	–	–

$\mu$ SR experiments were performed at the Swiss Muon Source (S $\mu$ S), Paul Scherrer Institute (PSI, Switzerland).

## 6. Overview of experimental studies of the gap in iron-based high- $T_c$ superconductors

Extensive experimental studies, involving point contact Andreev reflection spectroscopy (PCAR) [5]–[12], ARPES [3], [13]–[18], critical magnetic field ( $H_{c1}$ ) [19],  $\mu$ SR [4], [20]–[22], surface impedance (SI) [23], infrared spectroscopy (optics) [24, 25] and scanning tunnelling spectroscopy (STS) [26]–[29] measurements carried out on different iron-based superconductors, SmFeAsO $_{1-x}$ F $_x$  [5, 6, 11, 25, 26], LaFeAsO $_{1-x}$ F $_x$  [8], NdFeAsO $_{1-x}$ F $_x$  [9, 13, 16], Ba $_{1-x}$ K $_x$ Fe $_2$ As $_2$  [3, 4, 7, 10, 12, 14, 15, 17, 19, 20, 23, 24], BaFe $_{2-2x}$ Co $_{2x}$ As $_2$  [10, 18, 28, 29], Sr $_{1-x}$ K $_x$ Fe $_2$ As $_2$  [27], SrFe $_{2-2x}$ Co $_{2x}$ As $_2$  [22] and FeSe $_{0.85}$  [21], let us conclude that most of these systems exhibit two superconducting gaps—a small one with coupling constant  $2\Delta_{\text{small}}/k_B T_c \sim 2.5$  and a large one with  $2\Delta_{\text{large}}/k_B T_c \sim 7$  (see table 1 and figure 6). Some studies overlook one of the gaps (either small [13, 16, 24, 25, 27] or even the large one [5, 26]). In addition, many other measurements confirm unconventional multi-gap behaviour of iron-based superconductors [30]–[38].

Based on ARPES measurements one may not only state that different bands bear different gaps, but also reveal the complete momentum dependence of the gap magnitude—in BKFA the large gap opens on the inner  $\Gamma$ -barrel and the propeller-like structure around the X point, while the small gap opens only on the outer  $\Gamma$ -barrel [3, 14]. It is interesting to note that recent ARPES studies of the electron-doped compound BaFe $_{1.85}$ Co $_{0.15}$ As $_2$  have suggested that the smaller gap opens on the bands in the vicinity of X point, while the large one opens on the bands around  $\Gamma$  [18]. The anisotropy of the gap within one Fermi surface sheet has not been firmly established, although some evidence for small variations within the inner  $\Gamma$ -barrel ( $\sim 10\%$ ) was reported

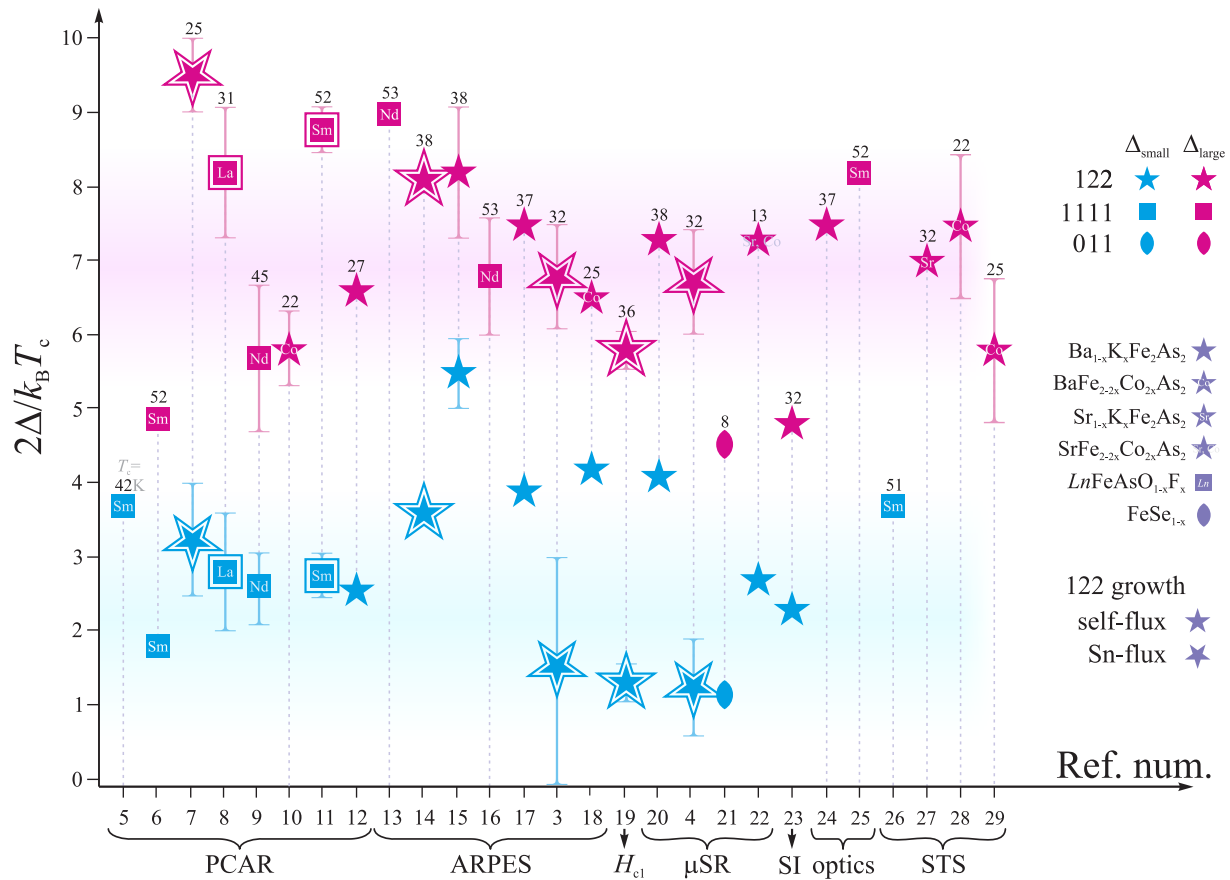


**Figure 6.** Coupling constant,  $2\Delta/k_B T_c$ , in iron arsenides, as revealed by different experimental techniques (refer to the main text for expansion of the abbreviations). In the figure, the points corresponding to the data taken on 122 (doped  $A\text{Fe}_2\text{As}_2$ ) systems are denoted by stars, points corresponding to 1111 (doped  $\text{LnFeAsO}$ ) systems are denoted by squares, and points corresponding to 011 ( $\text{FeSe}_{0.85}$ ) are denoted by spindle-like symbols. Stars, corresponding to the studies of  $\text{Sr}_{1-x}\text{K}_x\text{Fe}_2\text{As}_2$ , are marked by ‘Sr’, corresponding to  $\text{BaFe}_{2-2x}\text{Co}_{2x}\text{As}_2$ , are marked by ‘Co’, and corresponding to  $\text{SrFe}_{2-2x}\text{Co}_{2x}\text{As}_2$ , are marked by ‘Sr, Co’. For 1111 systems, the element  $\text{Ln}$  in the structural formula  $\text{LnFeAsO}_{1-x}\text{F}_x$  is given inside the squares. Critical temperature,  $T_c$  (K), is given as numbers above the symbols. Blue symbols correspond to the small gap, while maroon ones correspond to the large gap. Studies on the 122 crystals grown by the Sn-flux method are shown as overturned stars. Points corresponding to the most comprehensive and quality studies are marked by an extra frame. There are two superconducting gaps in these systems—the ‘small’ one and the ‘large’ one, although some studies overlook one of the gaps [5, 13, 16], [24]–[27].

[3, 15]. In addition, it is worthwhile noting that all of the above refers only to the magnitude (absolute value) of the gap. As suggested by nuclear magnetic resonance (NMR) and nuclear quadrupole resonance (NQR) studies, the order parameter changes sign between different Fermi surface sheets [30]–[32].

## 7. Conclusions

Recently, it was shown that ARPES allows one to explain and predict many macroscopic physical properties of the material that depend on the low-lying electronic structure—transport properties [42, 49, 50], propensity of the system to form additional order [51] and critical temperature of the superconducting transition [52]. In this paper, we have presented a calculation of the London penetration depth from ARPES data (to the best of our knowledge, it is the first calculation of such a kind). A comparison of the obtained results with direct  $\mu$ SR measurements has shown good agreement, which allows us to state that we have determined the robust momentum dependence of the superconducting gap in the bulk of BKFA. Namely, the gap distribution over the Fermi surface is consistent with that reported in our ARPES studies of this compound [3]—the gap is small ( $2\Delta_{\text{small}}/k_{\text{B}}T_{\text{c}} < 3$ ) on the outer  $\Gamma$ -barrel, and large on the other parts of the Fermi surface ( $2\Delta_{\text{large}}/k_{\text{B}}T_{\text{c}} = 6.8$ ). Furthermore, comparison with  $\mu$ SR measurements resulted in the improved estimate of the small gap magnitude—its coupling constant turned out to be  $\simeq 1$  instead of the previous  $< 3$ .

## Acknowledgments

This work is part of the FOR538 and was supported by the DFG under grants nos. KN393/4, KN393/12 and BO1912/2-1. We thank A N Yaresko for useful discussions and R Hübel, R Schönfelder and S Leger for technical support.

## Appendix

Integrals of the form

$$D(\Delta, \Sigma'', T) = \int_{-\infty}^{+\infty} \left( -\frac{\partial f_T(\omega)}{\partial \omega} \right) \left| \operatorname{Re} \frac{\omega + i\Sigma''}{\sqrt{(\omega + i\Sigma'')^2 - \Delta^2}} \right| d\omega \quad (\text{A.1})$$

often appear upon calculation of the different physical properties of the materials from their low-energy electronic structure. Unfortunately, the integration cannot be performed analytically; therefore it is useful to find a convenient approximating formula. For the practically important case of  $\Sigma'' = 0$ , the function  $D(\Delta, 0, T)$  can be approximated by an elementary function

$$M\left(\frac{\Delta}{k_{\text{B}}T}\right) = \frac{4}{(e^{(\Delta/2k_{\text{B}}T)} + e^{-(\Delta/2k_{\text{B}}T)})^2} \sqrt{\frac{\pi}{8} \frac{\Delta}{k_{\text{B}}T} + \frac{1}{1 + \frac{\pi}{8} \frac{\Delta}{k_{\text{B}}T}}}. \quad (\text{A.2})$$

The accuracy of such an approximation is better than 3% for the entire range of parameters  $\Delta$  and  $T$ :

$$-0.03 < \frac{D(\Delta, 0, T) - M(\Delta/k_{\text{B}}T)}{D(\Delta, 0, T)} < 0.015, \quad \forall \Delta, T > 0. \quad (\text{A.3})$$

**References**

- [1] Zabolotnyy V B *et al* 2009 *Nature* **457** 569
- [2] Zabolotnyy V B *et al* 2009 *Physica C* **469** 448
- [3] Evtushinsky D V *et al* 2009 *Phys. Rev. B* **79** 054517
- [4] Khasanov R *et al* 2009 *Phys. Rev. Lett.* **102** 187005
- [5] Chen T Y *et al* 2008 *Nature* **453** 1224
- [6] Wang Y *et al* 2009 *Supercond. Sci. Technol.* **22** 015018
- [7] Szabo P *et al* 2009 *Phys. Rev. B* **79** 012503
- [8] Gonnelli R S *et al* 2008 arXiv:0807.3149
- [9] Samuely P *et al* 2009 *Supercond. Sci. Technol.* **22** 014003
- [10] Samuely P *et al* 2009 arXiv:0902.2667
- [11] Gonnelli R S *et al* 2009 arXiv:0902.3441
- [12] Goll G *et al* 2009 Probing the superconductive energy gap of the iron pnictide superconductor  $\text{Ba}_{1-x}\text{K}_x\text{Fe}_2\text{As}_2$  by point-contact and scanning tunnelling spectroscopy *DPG meeting (Dresden)* <http://www.dpg-verhandlungen.de/2009/dresden/tt.pdf>
- [13] Liu C *et al* 2008 arXiv:0806.2147
- [14] Ding H *et al* 2008 *Europhys. Lett.* **83** 47001
- [15] Zhao L *et al* 2008 *Chin. Phys. Lett.* **25** 4402
- [16] Kondo T *et al* 2008 *Phys. Rev. Lett.* **101** 147003
- [17] Wray L *et al* 2008 arXiv:0808.2185
- [18] Terashima K *et al* 2008 arXiv:0812.3704
- [19] Ren C *et al* 2008 *Phys. Rev. Lett.* **101** 257006
- [20] Hiraishi M *et al* 2009 *J. Phys. Soc. Japan* **78** 023710
- [21] Khasanov R *et al* 2008 *Phys. Rev. B* **78** 220510
- [22] Khasanov R *et al* 2009 arXiv:0903.1270
- [23] Hashimoto K *et al* 2008 arXiv:0810.3506
- [24] Li G *et al* 2008 *Phys. Rev. Lett.* **101** 107004
- [25] Dubroka A *et al* 2008 *Phys. Rev. Lett.* **101** 097011
- [26] Millo O *et al* 2008 *Phys. Rev. B* **78** 092505
- [27] Boyer M C *et al* 2008 arXiv:0806.4400
- [28] Masee F *et al* 2008 arXiv:0812.4539v2
- [29] Yin Y *et al* 2009 *Phys. Rev. Lett.* **102** 097002
- [30] Kawasaki S *et al* 2008 *Phys. Rev. B* **78** 220506
- [31] Grafe H-J *et al* 2008 *Phys. Rev. Lett.* **101** 047003
- [32] Matano K *et al* 2008 *Europhys. Lett.* **83** 57001 (arXiv:0903.5098)
- [33] Mu G *et al* 2008 arXiv:0808.2941
- [34] Martin C *et al* 2009 arXiv:0903.2220  
Martin C *et al* 2009 arXiv:0902.1804
- [35] Gordon R T *et al* 2009 *Phys. Rev. Lett.* **102** 127004
- [36] Hashimoto K *et al* 2009 *Phys. Rev. Lett.* **102** 017002
- [37] Malone L *et al* 2008 arXiv:0806.3908
- [38] Yates K A *et al* 2009 *New J. Phys.* **11** 025015
- [39] Park J T *et al* 2009 *Phys. Rev. Lett.* **102** 117006
- [40] Goko T *et al* 2008 arXiv:0808.1425
- [41] Chandrasekhar B S and Einzel D 1993 *Ann. Phys.* **505** 535
- [42] Evtushinsky D *et al* 2008 *Phys. Rev. Lett.* **100** 236402
- [43] Gross F *et al* 1986 *Z. Phys. B* **64** 175
- [44] Rotter M, Pangerl M, Tegel M and Johrendt D 2008 *Angew. Chem. Int. Edn* **47** 7949

- [45] Mahan G D 1970 *Phys. Rev. B* **2** 4334
- [46] Sun G L *et al* 2009 arXiv:0901.2728
- [47] Inosov D S *et al* 2008 *Phys. Rev. B* **77** 212504
- [48] Koitzsch A *et al* 2009 *Phys. Rev. Lett.* **102** 167001
- [49] Evtushinsky D *et al* 2006 *Phys. Rev. B* **74** 172509
- [50] Narduzzo A *et al* 2008 *Phys. Rev. B* **77** 220502
- [51] Borisenko S V *et al* 2008 *Phys. Rev. Lett.* **100** 196402  
Inosov D S *et al* 2008 *New J. Phys.* **10** 125027  
Inosov D S *et al* 2009 *Phys. Rev. B* **79** 125112  
Inosov D S *et al* 2009 *Phys. Rev. Lett.* **102** 046401  
Borisenko S V *et al* 2009 *Phys. Rev. Lett.* **102** 166402
- [52] Dahm T *et al* 2009 *Nat. Phys.* **5** 217